Neuron
Article

Myosin IIb Regulates Actin Dynamics during Synaptic Plasticity and Memory Formation

Christopher S. Rex,[2] Cristin F. Gavin,[1,7] Maria D. Rubio,[1] Eniko A. Kramar,[2] Lulu Y. Chen,[4] Yousheng Jia,[2] Richard L. Huganir,[6] Nicholas Muzyczka,[5] Christine M. Gall,[3,4] Courtney A. Miller,[1,7] Gary Lynch,[2] and Gavin Rumbaugh[1,7,*]

[1]Department of Neurobiology and Evelyn F. McKnight Brain Institute, The University of Alabama at Birmingham, Birmingham, AL 35294, USA
[2]Department of Psychiatry and Human Behavior
[3]Department of Neurobiology and Behavior
[4]Department of Anatomy and Neurobiology
University of California, Irvine, CA 92697, USA
[5]Department of Molecular Genetics and Microbiology, University of Florida Genetics Institute, The University of Florida, Gainesville, FL 32610, USA
[6]Department of Neuroscience and Howard Hughes Medical Institute, The Johns Hopkins University School of Medicine, Baltimore, MD 21205, USA
[7]Present address: Department of Neuroscience, The Scripps Research Institute, Jupiter, FL 33458, USA
*Correspondence: grumbaug@scripps.edu
DOI 10.1016/j.neuron.2010.07.016

SUMMARY

Reorganization of the actin cytoskeleton is essential for synaptic plasticity and memory formation. Presently, the mechanisms that trigger actin dynamics during these brain processes are poorly understood. In this study, we show that myosin II motor activity is downstream of LTP induction and is necessary for the emergence of specialized actin structures that stabilize an early phase of LTP. We also demonstrate that myosin II activity contributes importantly to an actin-dependent process that underlies memory consolidation. Pharmacological treatments that promote actin polymerization reversed the effects of a myosin II inhibitor on LTP and memory. We conclude that myosin II motors regulate plasticity by imparting mechanical forces onto the spine actin cytoskeleton in response to synaptic stimulation. These cytoskeletal forces trigger the emergence of actin structures that stabilize synaptic plasticity. Our studies provide a mechanical framework for understanding cytoskeletal dynamics associated with synaptic plasticity and memory formation.

INTRODUCTION

Structural and functional plasticity of synapses underlies information storage in the brain (Segal, 2005). As such, elucidating the cellular and molecular processes supporting synaptic plasticity may reveal new targets for treating memory dysfunction. Actin filaments are the major cytoskeletal component of dendritic spines and appear to regulate both steady-state and plastic processes in CA1 pyramidal neurons (Allison et al., 1998; Fukazawa et al., 2003; Krucker et al., 2000; Matsuzaki et al., 2004; Matus et al., 1982). Disrupting actin filaments in CA1 following memory acquisition promotes amnesia (Fischer et al., 2004), while inhibiting actin polymerization selectively disrupts the maintenance of synaptic plasticity (Honkura et al., 2008; Krucker et al., 2000; Rex et al., 2009). Therefore, elucidating the regulatory mechanisms that influence dynamic actin will illuminate critical aspects of synaptic plasticity and memory formation, and harnessing the potential of these mechanisms could lead to novel treatments for memory disorders.

Long-term potentiation (LTP) of excitatory synaptic responses is a cellular phenomenon widely regarded to be the substrate of multiple forms of learning and can be used to investigate the molecular events underlying memory acquisition and maintenance (Martin et al., 2000; Pastalkova et al., 2006; Sigurdsson et al., 2007; Whitlock et al., 2006). The dominant cellular model of memory formation is LTP in area CA1 of the adult hippocampus. This form of synaptic plasticity is accompanied by changes in the morphology of dendritic spines and synapses (Lang et al., 2004; Lee et al., 1980; Matsuzaki et al., 2004) and a growing body of evidence suggests that these changes involve dynamic reorganization of the actin cytoskeleton (Honkura et al., 2008; Lin et al., 2005a; Okamoto et al., 2004). The role of actin polymerization in modifying spine structure is consistent with the long-standing idea that synaptic potentiation is often dependent on the spine cytoarchitecture (Matus, 2000). Taken together, these ideas suggest that the dynamic reorganization of actin filaments may represent an early step in information encoding. Therefore, identifying the molecules that trigger these cytoskeletal rearrangements may uncover novel mechanisms of memory formation. However, the molecular mechanisms at synapses that drive the emergence of new F-actin structures during circuit plasticity are unknown.

The actin cytoskeleton is comprised of several distinct structures, including stable bundles, dynamic bundles, single filaments, and smaller structures defined as "arcs." Conceptual

approaches to understanding the dynamic nature of the actin cytoskeleton in neurons has focused on actin-binding proteins that regulate treadmilling, branching, and stabilization of individual filaments (Lynch et al., 2007; Rex et al., 2009; Star et al., 2002). However, evidence from nonneuronal cells and immature neurons indicate that the actin cytoskeleton is actually a multiordered, dynamic structure capable of self-regulation through mechanical forces mediated by local network contractions (Mogilner and Keren, 2009). These actin-mediated actin dynamics, combined with the activity of filament binding proteins, provide the necessary complexity for dynamic changes to neuronal morphology and cellular growth. Local actin network contractions provide the force necessary to trigger remodeling of larger F-actin structures, such as turnover of bundled fibers that provide the drive for rapid morphological changes in growth structures (Medeiros et al., 2006). Considering that multiple pools of F-actin exist in dendritic spines (Honkura et al., 2008; Star et al., 2002), we hypothesized that forebrain excitatory synapses contain a similarly complex and dynamic system of cytoskeletal reorganization mechanisms.

In immature neurons, myosin II directly alters cytoskeletal dynamics through ATPase-driven contraction of actin networks (Lin et al., 1996; Medeiros et al., 2006). This property is in stark contrast to other forms of neuronal myosin, such as the cargo motors myosin V and VI. Although these vesicle-transport motors have received much attention in recent years for their roles in neuronal polarity and AMPA receptor trafficking (Correia et al., 2008; Lewis et al., 2009; Osterweil et al., 2005; Wang et al., 2008), myosin II's motor capacity has been co-opted by growth structures to directly regulate actin dynamics (Vallee et al., 2009; Vicente-Manzanares et al., 2009). For instance, myosin II-mediated contractility of actin networks in growth cones causes shearing of large actin bundles, which leads to the disassembly of the resulting small F-actin structures (Medeiros et al., 2006). These monomeric globular (G)-actin molecules are then added to the growing end of actin bundles, resulting in growth cone propulsion. Acutely inhibiting myosin II arrests this retrograde flow of actin, resulting in growth cone collapse and inhibition of neurite elongation. Thus, paradoxically, myosin II is capable of indirectly causing both actin polymerization and depolymerization in the neuronal growth cone. Indeed, it is believed that activity of this motor imparts the actin cytoskeleton with the necessary complexity to drive the dynamics of growth structures (Backouche et al., 2006).

Myosin II is also abundantly expressed in the adult nervous system, with three distinct isoforms of myosin II heavy chains present in isolated postsynaptic densities of mature forebrain synapses (Cheng et al., 2000, 2006; Miyazaki et al., 2000). Disrupting myosin II activity in cultured neurons alters the development of dendritic spines (Ryu et al., 2006; Zhang et al., 2005), though it is unknown if myosin II regulates actin networks in mature synapses. And further, the role of myosin II in plastic processes, such as LTP and memory formation, remains completely unexplored. Considering the importance of actin dynamics at excitatory synapses in the hippocampus, we hypothesized that myosin II-mediated mechanical forces in dendritic spines are necessary for the emergence of F-actin structures that stabilize synaptic plasticity and promote memory formation.

Indeed, we demonstrate here that myosin II is a necessary component of hippocampus-dependent memory formation and synaptic plasticity in the mature nervous system. We found that myosin II function was upstream of actin polymerization and filament stabilization, consistent with the role of this protein complex as a regulator of dynamic actin structures. Myosin II activity was required for the initial stabilization of LTP at CA1 synapses, a period marked by rapid actin filament synthesis in response to synaptic NMDAR activation. Both actin polymerization and myosin II activity initiated by synaptic stimulation were necessary for the stabilization of synaptic plasticity over identical time courses, suggesting their activities are highly synchronized to convert newly potentiated synapses from a labile to stable state. Taken together, our data support a model where myosin IIb motor activity regulates NMDAR-driven actin network dynamics and show that this mechanism is necessary for synaptic plasticity and memory formation.

RESULTS

Myosin IIb Is Essential for Synaptic Stability and the Emergence of Newly Synthesized Actin Structures

To test the idea that myosin IIb is a critical regulator of synaptic plasticity, we developed a method that could selectively target myosin II motors in the adult hippocampus. rAAV2 virus particles psuedotyped with rAAV5 coat proteins (rAAV2/5) are especially effective tools for selectively transducing hippocampal neurons in vivo (Burger et al., 2004). We utilized a strong enhanced green fluorescent protein (eGFP) expressing rAAV2/5 virus in order to optimize injection location and volume. A single injection of rAAV2/5 particles resulted in selective expression of eGFP in dorsal CA1 that spread as much as a millimeter in the rostral-caudal axis (Figure 1A). eGFP was expressed at very high levels in dendrites, most neurons in the dorsal CA1 were positive for eGFP, and transgene expression did not disrupt the cellular layers (Figure 1B). We next designed and packaged rAAV particles that express shRNAs in vivo that selectively target the heavy chain of myosin IIb, *MyH10*. These particles were in an identical virus package (rAAAV2/5), though they contained two expression cassettes. One drove weak wtGFP expression, while the other drove expression of shRNAs (control shRNA or MyH10-specific shRNA). Weak wtGFP expression allowed us to locate areas of CA1 with the highest levels of transduction, which facilitated LTP studies (Figure 1C). MyH10-shRNAs driven by these particles caused a 5-fold reduction in MyH10 expression from homogenates collected from dorsal hippocampus relative to control shRNA hippocampal samples (Figure S1).

We next unilaterally injected either control or MyH10-shRNA virus into the dorsal hippocampus of adult rats to assess the physiological consequences of reducing MyH10 expression. The opposite, naive hemisphere provided critical internal controls for virus injection and hairpin expression. Thirty days after injection, which is the time necessary to reach maximum expression of packaged nucleic acids using rAAV2/5 particles (Burger et al., 2004), we prepared acute hippocampal slices from these animals. There were no gross structural differences between the injected and naive hemispheres in either virus group. The size and shape of field synaptic potentials elicited by

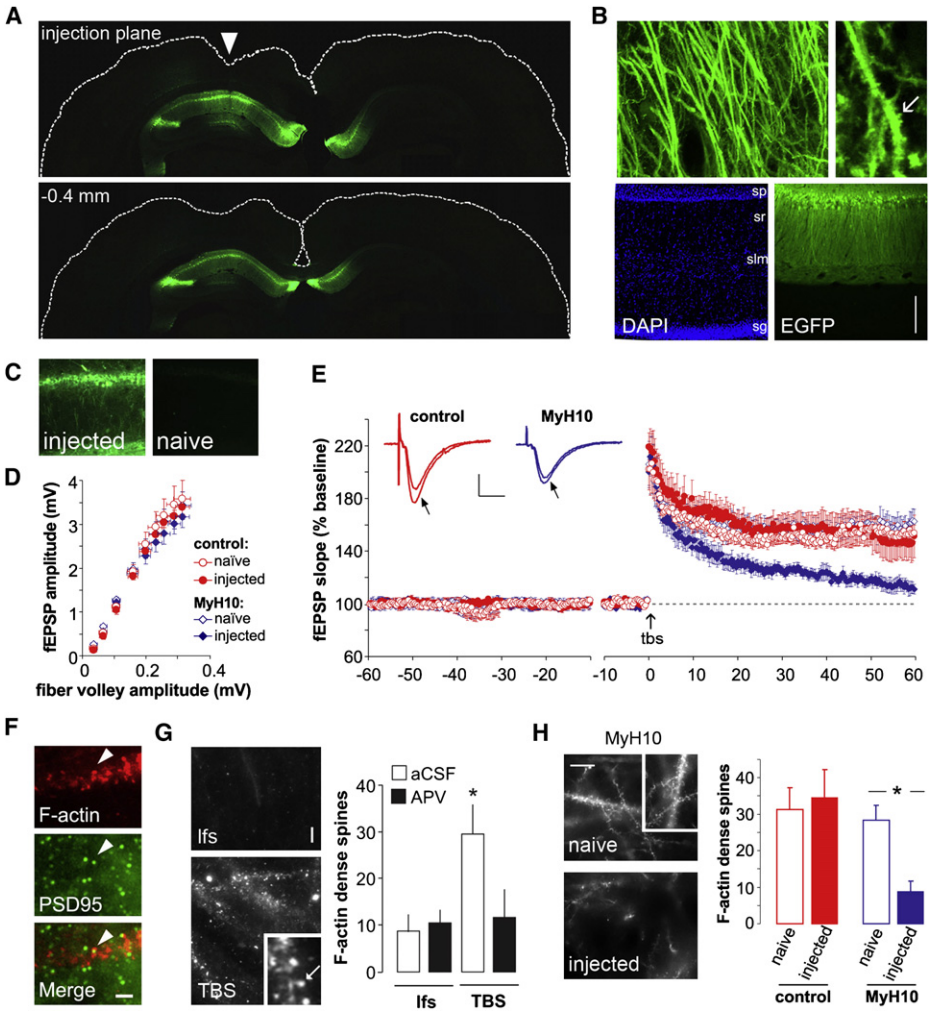

Figure 1. Myosin IIb Is Required for Stable LTP and Activity-Related Spine Actin Polymerization

(A) An adult rat received a unilateral dorsal hippocampal injection (3 μl) of a recombinant adeno-associated virus (rAAV) construct expressing an optimized eGFP cassette. Arrow represents injection needle track.

(B) Higher magnification of sections shown in (A) (with inclusion of a DAPI costain). Arrow denotes clearly visible dendritic spines. Scale bar: 100 μm, for lower panels. sp, stratum pyramidale; sr, stratum radiatum; slm, stratum lacunosum moleculare.

(C) Photomicrographs of wtGFP expression in dorsal hippocampal slices prepared from injected and contralateral (naive) hemispheres following unilateral injections (1 μl) of a rAAV coexpressing MyH10 shRNA and wtGFP. Images were collected from fixed slices following electrophysiological recordings. Scale bar: 20 μm.

(D) Input-output relationships for synaptic responses in hippocampus CA1b of slices prepared from dorsal hippocampus 30–40 days after virus injections. No differences between groups were observed ($p > 0.05$, one-way RM-ANOVA; n = 4 animals/group).

(E) Baseline synaptic responses were stable for up to 50 min of recording (minutes −60 to −10) in all groups (n = 4 animals/group). Break in x axis indicates I/O curve collection period (<5 min). LTP induction (1–2 min post-TBS) was equivalent between all groups ($p > 0.05$), but slices collected from hemispheres injected with *MyH10* shRNA failed to express stable LTP ($p = 0.02$, two-way RM-ANOVA for 30–50 min post-TBS). Calibration: 0.5 mV, 10 ms.

(F) Photomicrographs show in situ labeling of F-actin by Alexa 568-phalloidin in a proximal dendrite from a CA1 pyramidal neuron in an adult slice. Densely labeled structures were colabeled with postsynaptic density-95 (PSD95) immunoreactivity (arrowhead) indicating that these are dendritic spines. Scale bar: 2 μm.

(G) Spine F-actin labeling in the region of electrophysiological recording for slices receiving baseline stimulation (Ifs) or collected after TBS. Slices receiving TBS exhibited numerous densely labeled spine heads (arrow in inset). Scale bar: 5 μm, 1 μm for inset. Preincubations of 50 μM APV (closed bars) or aCSF (open) for 30 min prior to and continuing through in situ phalloidin labeling blocked the TBS-induced increase in densely phalloidin-labeled spines (*$p < 0.05$ for TBS versus Ifs, Tukey's HSD; $p > 0.05$ for Ifs/APV versus TBS/APV).

(H) Photomicrographs show F-actin in str. radiatum labeled in situ with Alexa 594-phalloidin following LTP induction by TBS in slices prepared from *MyH10* shRNA-injected animals (injected) or the contralateral hemisphere (naive). Quantification of densely labeled spines in slices that received TBS showed that naive and control-injected, but not *MyH10* shRNA-injected, hemispheres exhibited numbers consistent with TBS induction ($p < 0.05$, ANOVA; n = 3 animals/group; *$p < 0.05$, Tukey's HSD).

Error bars represent SEM.

stimulation of Schaffer-collateral afferents were equivalent among all groups, indicating that ~80% reduction of MyH10 from the adult CA1 does not adversely affect basic synaptic function (Figure 1D). The initial potentiation following LTP induction was comparable across all slices, but there was a marked and selective deficit in LTP stability from slices expressing the MyH10 hairpin compared to naive (no injection) slices from the same animal (Figure 1E). Importantly, there was also no effect of the control shRNA on LTP stability (Figure 1E), indicating that the virus injection procedure and expression of exogenous noncoding RNAs do not affect LTP at these synapses. These data demonstrate that myosin IIb expression is critically important for stabilization, but not induction, of early LTP.

Myosin II is a ubiquitous regulator of complex actin structures (Mogilner and Keren, 2009), and F-actin dynamics are regulated by LTP induction (Fukazawa et al., 2003; Lin et al., 2005b; Okamoto et al., 2004). To test the idea that myosin II regulates actin dynamics during LTP, we used a technique that labels F-actin synthesis in situ in response to LTP-inducing synaptic stimulation (Lin et al., 2005a; Rex et al., 2009). This method exploits the fact that neurons, unlike other cell types, are permeable to phalloidin in a dose-dependent manner (Lin et al., 2005a; Rex et al., 2009). Spine-like structures labeled by phalloidin in response to theta burst stimulation (TBS) colocalized with PSD-95 (Figure 1F) and this increase in spine F-actin was blocked by NMDAR antagonists (Figure 1G). Also, phalloidin labeling intensity increased as a function of phalloidin concentration in slices (Figure S2). This technique was applied to the slices obtained from MyH10-shRNA-injected animals used for LTP studies (see Figure 1E). One hour after LTP induction, there were no differences in the density of phalloidin labeling found in spines within the zone of synaptic potentiation for control-virus-injected and naive hemispheres. Importantly, this labeling was equivalent to data from past studies (Lin et al., 2005a; Rex et al., 2009), and these groups were not significantly different from each other (Figure 1H). In contrast, slices expressing MyH10-shRNAs demonstrated significantly depressed levels of activity-induced spine F-actin structures (Figure 1H). These data confirm that myosin IIb is necessary for the long-term expression of actin filaments following LTP induction and indicate that this motor protein regulates actin dynamics at synapses.

Myosin II ATPase Activity Stabilizes Synaptic Plasticity by Regulating Postinduction Actin Dynamics

To further investigate the mechanism of myosin II function during synaptic plasticity, we hypothesized that the myosin II complex was a target of NMDAR-activated signaling pathways initiated by LTP induction. Therefore, we probed hippocampal slices for a structural correlate of myosin II ATPase activity. Myosin II is a hexameric protein complex containing dimerized heavy chains, as well as two copies of a smaller regulatory light chain (MLC20). While the heavy chains possess a motor domain, myosin II activity is activated by phosphorylation of MLC20^{S19} (Vicente-Manzanares et al., 2009). Phosphorylation of MLC20^{S19} (p-MLC20^{S19}) is the primary signal that activates the heavy-chain motor of nonmuscle myosin II (Even-Faitelson et al., 2005; Goeckeler et al., 2000; Hirano et al., 2004; Matsumura, 2005; Vicente-Manzanares et al., 2009; Zeng et al., 2000). To investigate myosin II phosphorylation at synapses, we used two distinct approaches. We first tested the idea that NMDAR activation of a pure synaptoneurosomal preparation could induce p-MLC20^{S19}. Indeed, application of 100 μM NMDA induced p-MLC20^{S19}, while also inducing cofilin phosphorylation (Figure 2A). We then asked if NMDARs targeted myosin phosphorylation through Rho-GTPase signaling. Preincubation with the ROCK inhibitor, H1152 (1 μM), complexly blocked both myosin and cofilin phosphorylation by NMDA (Figure 2A). We next sought to determine if LTP induction caused MLC phosphorylation. We did this by exploiting a recently described method for probing phospho-protein levels at individual synapses in acute slices following theta burst stimulation (Chen et al., 2007; Rex et al., 2009). We induced LTP at Schaffer-collateral synapses and then labeled the tissue with antibodies for pMLC20^{S19} and PSD95. This method resulted in punctate labeling of pMLC that colocalized with PSD95-positive (+) elements of similar size (Figure 2B). Automated identification of synaptic pMLC20^{S19} within the zone of synaptic potentiation indicated a modest effect of TBS on PSD95-positive synapses containing dense pMLC20^{S19}; but optimal results were obtained by rapid extraction of soluble proteins prior to fixation (Medeiros et al., 2006). Under these conditions, slices receiving TBS exhibited roughly 3-fold greater numbers of PSD95-positive synapses containing dense pMLC20^{S19} versus slices receiving control stimulation (Figure 2B). Pretreating slices with APV (50 μM, 30 min) prevented TBS-induced increases in pMLC20^{S19} at synapses, confirming that this effect was dependent upon NMDA receptor activation. In addition, perfusion of a ROCK inhibitor, which prevents LTP stabilization and F-actin synthesis (Rex et al., 2009), also completely blocked TBS-induced synaptic pMLC20^{S19} (Figure 2B). These data provide evidence that NMDA receptor stimulation and LTP induction triggers one or more second messenger systems that activate the myosin II motor.

To determine the temporal dynamics of myosin II activity during LTP and to directly test the hypothesis that its force-generating activity regulates synaptic plasticity, we applied the specific inhibitor of myosin II ATPase activity, Blebbistatin (Blebb) (Straight et al., 2003), to adult hippocampal slices. Following Blebb application, we recorded synaptic responses resulting from stimulation of Schaeffer collateral (SC) inputs to CA1 neurons (str. radiatum). This compound selectively inhibits the myosin II ATPase motor without affecting the function of other classes of myosin (e.g., myosin V, myosin VI) (Limouze et al., 2004). Blebb did not alter basic properties of synaptic transmission or baseline responses during hour-long field recordings (Figures 3A and 3B) and had no effect on spine morphology (Figure S3). Strikingly, Blebb caused a total disruption of TBS-induced LTP at (SC)-CA1 synapses (Figure 3C). Additionally, Blebb treatment did not block initial potentiation (<1 min post-TBS) or acute responses to the burst stimulation (Figure S4A) but caused fEPSP slopes to return to baseline levels within 15 min (Figure 3C), suggesting that Blebb alters LTP during the immediate postinduction *stabilization* period. We further confirmed that Blebb was not disrupting basic aspects of neuronal excitability that are required for TBS-induced LTP induction (Figure S4B). Importantly, the disruption of E-LTP

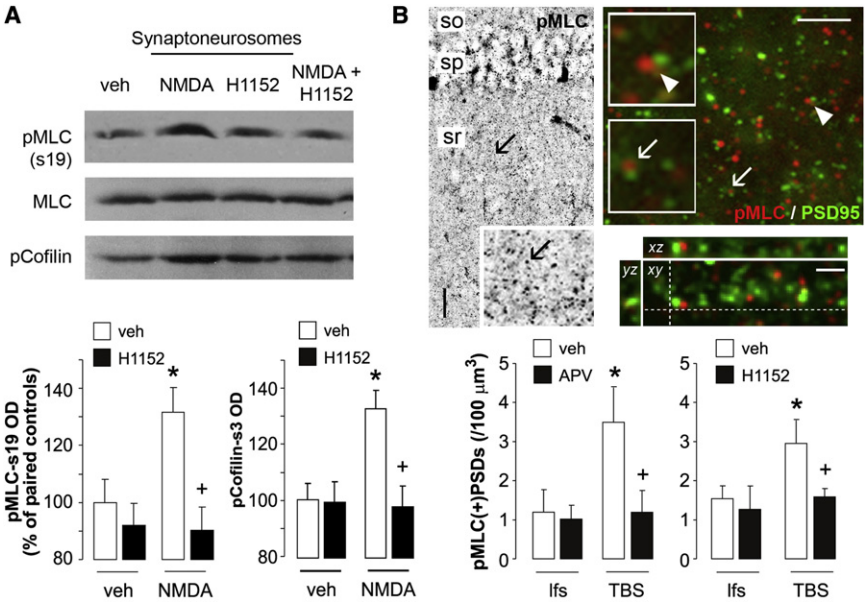

Figure 2. Myosin Light Chain Phosphorylation Is Triggered by NMDA Receptor Activation and LTP Induction

(A) Synaptoneurosomes were prepared from adult rats (4–6 weeks) and treated with NMDA (100 μM) or vehicle (veh) for 5 min. Blots (top) show immunoreactivity for phospho-myosin light chain (pMLC), total MLC, or phospho-cofilin. NMDA induced pMLC and pCofilin as assessed by quantification of optical densities (OD) and this was blocked by 5 min pretreatment with the ROCK inhibitor H1152 (1 μM) (*$p < 0.05$ versus veh/veh; +$p < 0.05$ versus NMDA/veh, Tukey's HSD; n = 5–6/group).

(B) Adult hippocampal slices received TBS or control stimulation (lfs) and were collected 5–7 min later for pMLC and PSD95 double immunolabeling. Following electrophysiology, slices were processed for tissue extraction using 2%–3% Triton X-100 in light fixation and cytoskeleton stabilizing media. (Upper left) Intensity-inverted deconvolution photomicrograph shows distribution of punctate labeling for pMLC throughout area CA1. Arrow indicates same puncta in low-magnification image and high-magnification inset. Scale bar: 10 μm, 5 μm for inset. so, stratum oriens; sp, stratum pyramidale; sr, stratum radiatum. (Upper right) Localization of pMLC+ and PSD95+ elements. Arrow and arrowhead indicate associated elements from the respective labels identified as pMLC+ PSDs. Scale bar: 5 μm, 2 μm for insets. (Middle right) Three-dimensional projections of deconvolved z-stack. Dotted lines indicate planes visualized for xz and yz. (Bottom) Counts of pMLC+ PSDs in the region of physiological recording for slices receiving TBS or lfs in the presence of 50 μM APV (30 min) or vehicle (veh). A similar pattern of results was obtained when LTP was induced in the presence of H1152 (200 nM; 30 min) (*$p < 0.05$ versus veh/lfs; + $p < 0.05$ versus veh/TBS; n = 9–14/group for APV study, n = 7–9/group for H1152 study). Error bars represent SEM.

maintenance by myosin II's ATPase inhibitor was similar to the effect of shRNAs targeting myosin IIb expression (Figure 1E), indicating that disrupting expression of myosin IIb and blocking myosin II motor activity have similar effects on the stabilization of synaptic plasticity. We confirmed that Blebb's effect on LTP was not due to presynaptic actions using two measures of presynaptic transmitter release probabilities, paired-pulse facilitation and miniature EPSC frequency (Figures 3D–3E). To test if this inhibitor is a nonselective blocker of synaptic plasticity, we perfused Blebb while evoking mossy-fiber responses in area CA3 str. lucidum. Synaptic potentiation induced at mossy fiber-CA3 synapses in the presence of an NMDA receptor antagonist was unaffected by identical Blebb treatments (Figure 3F). This synaptic potentiation was accompanied by a decrease in paired-pulse facilitation, supporting the suggestion that mossy fiber potentiation is mediated by presynaptic facilitation of release probability (Zalutsky and Nicoll, 1990), in contrast to postsynaptic F-actin reorganization processes observed in CA1 synapses.

We next explored the hypothesis that myosin II motor activity during the LTP postinduction period is necessary for stabilizing synaptic plasticity. To directly test this idea, we applied Blebb locally at different times after LTP induction (Figure 4A). Application of the inhibitor beginning 30 s, but not 10 min, after TBS, prevented the stabilization of potentiated fEPSPs. The window of Blebb's effective disruption of LTP closely matches dynamics of actin polymerization triggered by TBS (Kramár et al., 2006; Rex et al., 2009), suggesting that myosin II may play a role in actin polymerization during LTP induction. Therefore, we next performed identical LTP experiments with the actin filament assembly blocker, Latrunculin A (LatA). Strikingly, LatA perfusion produced time-dependent disruptions in LTP stability that were nearly identical to that of Blebb (Figure 4B).

The above data suggest that myosin II ATPase activity is involved in postinduction LTP processes that converge on F-actin synthesis, perhaps explaining how the myosin II motor contributes to LTP stability. To directly test this assertion, we perfused Blebb or LatA either 30 s, 2 min, or 10 min after LTP induction and then labeled F-actin structures by in situ phalloidin labeling (Figure 4C). Similar to our LTP studies, local infusions of each compound to slices also demonstrated identical effects on F-actin synthesis during LTP (Figures 4D and 4E). Specifically, each infusion disrupted TBS-induced F-actin levels when applied as early as 30 s after LTP induction, while these compounds had no effect on F-actin when applied 10 min postinduction. These results exhibit remarkable temporal parallels to Blebb's disruption of LTP (Figure 3A). Considering the near-identical effects of Blebb and LatA on both LTP stabilization and F-actin synthesis during LTP, these results strongly support the idea that myosin II motor activity is required for F-actin synthesis that is initiated by LTP induction.

It is possible that myosin II activity is involved in de novo formation of these specialized F-actin structures. Alternatively, myosin II may have little to do with synthesis, but is actually required to stabilize newly made F-actin structures. In order to explore these ideas, we first needed to measure the time course of actin polymerization following LTP induction in acutely prepared slices (Figure 5A). We did not detect newly synthesized

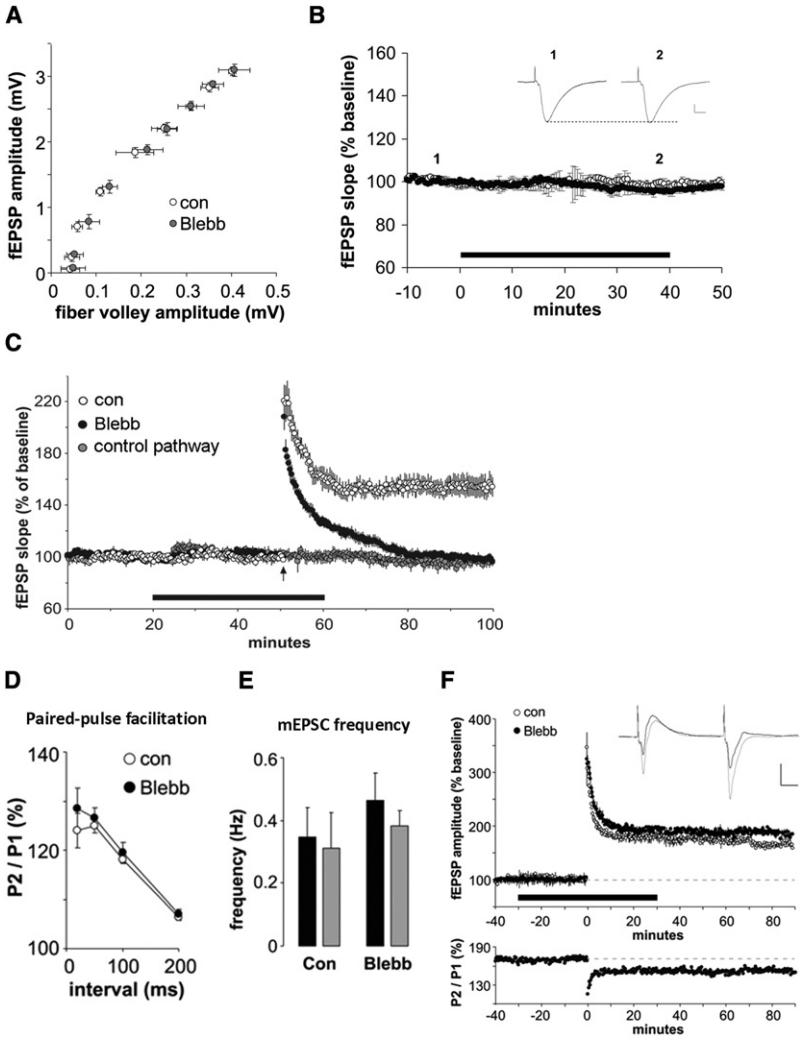

Figure 3. Myosin II ATPase Activity Is Required for NMDAR-Dependent Synaptic Plasticity

Low concentration of blebbistatin (10 μM) was bath applied to adult hippocampal slices.

(A) Blebbistatin (Blebb; gray symbols) applied for 1 hr had no effect on field response input-output relationships in Schaffer collateral-CA1 synapses ($p > 0.05$, RM-ANOVA; $n = 4$/group). In all subsequent experiments that use blebbistatin, the inactive enantiomer was always used as a control (*con*).

(B) Field potentials recorded in CA1 were unaffected by 40 min bath infusion (bar) of 10 μM of inactive (open) or active (closed symbols) blebbistatin ($p > 0.6$, RM-ANOVA). Inset shows representative fEPSPs prior to (1) and during (2) active blebbistatin wash-in. Calibration bar: 0.5 mV, 5 ms.

(C) Infusion of blebbistatin blocked stable formation of LTP ($p < 0.01$ versus control; RM-ANOVA) at CA3-CA1 synapses induced by TBS (arrow), but did not affect its immediate induction ($n = 7$/group). Control pathway (gray) was unaffected by blebbistatin treatment.

(D) Paired-pulse facilitation (P2/P1), expressed as the percent increase in response amplitude of pulse 2 versus pulse 1, was assessed in CA1 str. radiatum at 20, 50, 100, and 200 ms interpulse intervals. Blebbistatin infusion had no effect compared to control compound ($n = 5$/group).

(E) Summary of mEPSC frequencies recorded before (closed bars) and after (gray) 30 min infusion of blebbistatin. The drug had no effect on either measure ($n = 8$/group).

(F) Transmission at mossy fiber-CA3 synapses in the presence of 50 μM APV was not affected by 10 μM blebbistatin treatment. Mossy fiber potentiation (time 0) was accompanied by presynaptic facilitation indicated by a 20% reduction in PPF (50 ms interpulse interval; lower graph). The magnitude of mossy fiber potentiation was not different between blebbistatin- and control-treated slices ($n = 4$/group). (Inset) Overlaid baseline (black) and 30 min post-HFS (gray) MF-CA3 paired-pulse response traces. Calibration: 1 mV, 10 ms.

Error bars represent SEM.

F-actin structures 30 s after TBS, although synaptic responses are nearly doubled at this time point. However, changes were evident by 2 min and persisted at similar levels for at least 1 hr. With this precise knowledge of the time course of F-actin emergence during this early stabilization period of LTP, we could now test if myosin II motor activity is involved in the synthesis or stabilization of these actin structures. If myosin II is involved in filament stabilization, then an increase in F-actin labeling should be detectable at early time points but then rapidly dissipate. Therefore, we tested myosin II's contribution to the emergence of spine F-actin by applying Blebb for 30 min prior to TBS and harvesting at early time points. Blebb prevented TBS-induced increases in F-actin labeling at all time points (Figure 5B), indicating that new, stabilized F-actin structures did not emerge post-TBS. It is possible that Blebb has indirect effects on these F-actin structures by disrupting signal transduction pathways believed to target actin filament assembly in the minutes following LTP induction (Chen et al., 2007; Rex et al., 2009). Therefore, we labeled slices receiving TBS or control stimulation of Schaffer collaterals with antisera against phosphorylated cofilin (p-cofilin), a critical actin filament disassembly enzyme, as well as PSD95, to identify postsynapses (Chen et al., 2007). Pretreatment with Blebb failed to block TBS-induced p-cofilin at excitatory synapses (Figures 5C and 5D). We also confirmed that LatA did not disrupt this signaling pathway during TBS (data not shown). Slices treated with Blebb for 60–90 min also failed to exhibit decreased levels of p-cofilin as assessed by western blot analysis (data not shown). These results indicate that Blebb does not disturb actin filament generation by disrupting a primary signaling cascade targeting LTP-related actin filament assembly. Interestingly, these data also indicate that p-cofilin triggered by TBS is independent of actin polymerization in spines.

To directly address the question of whether or not myosin II contributes to actin filament assembly, we used fluorescence recovery after photobleaching (FRAP) in combination with Blebb to examine actin turnover in spines of dissociated neurons. The inhibitor had no effect on treadmilling rate but did significantly expand the pool of stable actin in spines, and this effect was proportional to the concentration of the inhibitor (Figures 5E

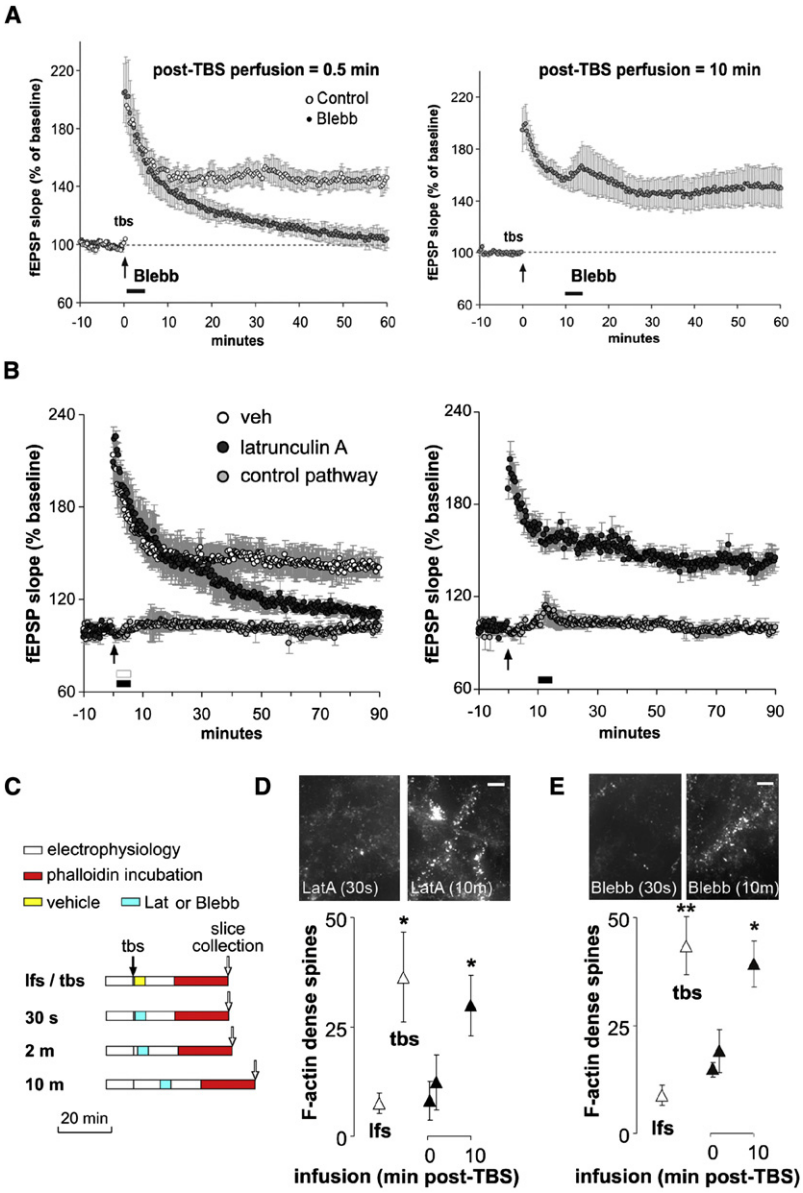

Figure 4. Myosin II Participates in Actin-Mediated Processes during the Immediate Stabilization of LTP

(A) (Left panel) Short-duration (4 min) local infusion (bar) of 10 μM blebbistatin (Blebb; closed symbols) or control compound (con; open symbols) beginning 30 s after TBS (arrow) prevented stable synaptic potentiation. The inactive compound (open symbols) did not affect LTP ($p < 0.01$, RM-ANOVA; n = 9/group). Blebbistatin applied 10 min post-TBS (right panel) did not affect stable synaptic potentiation (n = 10).

(B) (Left panel) Local transient infusion (bar) of 0.2 μM latrunculin A (closed symbols) beginning 30 s after TBS (arrow) had no immediate effect but disrupted potentiation compared to vehicle controls (open symbols) ($p < 0.001$; RM-ANOVA; n = 10–12/group). Control pathway (gray circles) was unaffected by the infusions or TBS. (Right panel) Latrunculin A applied 10 min post-TBS failed to disrupt LTP (n = 7).

(C) Schematic shows local infusion and in situ phalloidin labeling paradigm.

(D) Representative photomicrographs show labeled F-actin from slices receiving local infusions of latrunculin A (LatA) beginning 30 s (left) or 10 min post-TBS (right). Plot shows F-actin+ spine quantification from slices receiving local transient infusions of 0.2 μM latrunculin A (closed symbols) or vehicle (open). Latrunculin blocked the induction of densely phalloidin-labeled spines when applied 30 s or 2 min, but not 10 min, after initiating LTP. (*$p < 0.05$, Tukey's HSD versus lfs; n = 8–11/group.)

(E) Experiments performed identically to those in (D) but substituting local infusions of 10 μM blebbistatin (*$p < 0.05$, **$p < 0.01$, Tukey's HSD versus lfs; n = 5–7/group).

Scale bars in (D) and (E): 5 μM. Error bars represent SEM.

and 5F). Thus, myosin II activity directly contributes to the dynamic turnover of stable filaments at synapses. These data suggest that myosin ATPase activity is not contributing directly to actin filament elongation but is instead important for establishing an equilibrium between stable and unstable filaments within dendritic spines. We propose that this balance is essential for the production of de novo actin structures during LTP induction.

If myosin II activity is upstream of, and necessary for, actin filament polymerization, then pharmacologically inducing these events may protect synapses from disruption by myosin II inhibition. Jasplakinolide (JASP) potently induces actin filament synthesis (Allison et al., 1998; Holzinger, 2009; Okamoto et al., 2004) and protects LTP from disruption (Rex et al., 2009). As such, this compound is an ideal tool for testing myosin II-actin processes during LTP. For this experiment, we monitored the effectiveness of Blebb during the postinduction period of LTP with and without JASP pretreatments. JASP perfusion into hippocampal slices induced a slight rundown of synaptic responses (Figures 5G and 5H). However, when the stimulus strength was increased so as to return synaptic potentials to pre-JASP levels, we observed no effect of the compound on the initial expression or stability of LTP relative to control recordings. In addition, JASP perfusion (0.2 mM) did not alter burst responses arising from LTP induction or paired-pulse facilitation (Figure S5). Interestingly, when Blebb was infused 30 s after TBS into JASP-pretreated slices, there was no effect on LTP stability (Figure 5). Importantly, in parallel experiments, Blebb treatment alone disrupted LTP stability in vehicle pretreated slices, confirming our initial findings (Figures 3C and 4A). As such, these data support the hypothesis that myosin II activity is upstream of actin filament polymerization that serves to stabilize synaptic plasticity.

Myosin IIb Expression and Motor Activity Are Essential for Long-Term Memory Consolidation

LTP at CA1 synapses occurs in response to associative training (Fedulov et al., 2007; Roman et al., 1987; Whitlock et al., 2006),

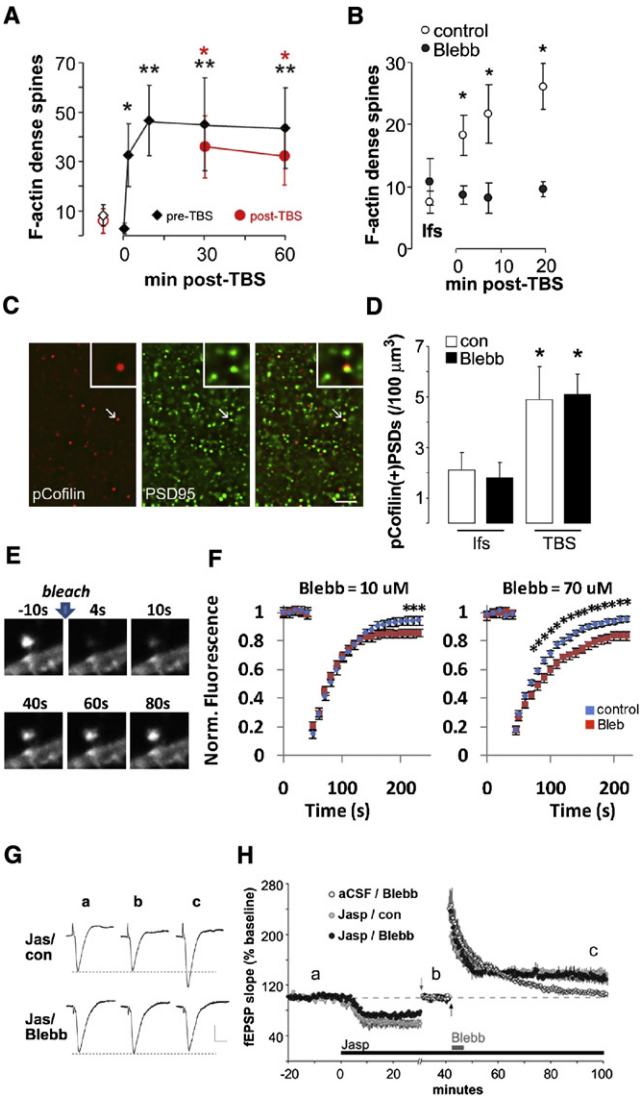

Figure 5. Myosin II ATPase Activity Is Required for LTP-Related Dendritic Spine Actin Polymerization

(A) Plot shows quantification of F-actin+ spines labeled in situ prior to (pre-; black diamonds) TBS and slices collected 0.5, 2, 7, 30, and 60 min after TBS. Similar results were obtained with post-TBS in situ phalloidin incubation (red circles) for slices collected at 30 and 60 min (**$p < 0.01$, *$p < 0.05$; Tukey's HSD versus control stimulation [lfs]; n = 8–12/group).

(B) Slices were labeled for F-actin prior to induction of LTP by theta burst stimulation and harvested 2, 7, or 20–30 min post-TBS. Bath applications (40 min, 10 μM) of the active (Blebb), but not inactive (con), isoform of blebbistatin prevented TBS-induced increases in F-actin+ spine density in the region containing activated synapses (*$p < 0.05$, Tukey's HSD; n = 5–7/group).

(C and D) Micrographs show double-immunofluorescence for phosphorylated (p) Cofilin and PSD95 in slices collected 5–7 min post-TBS or lfs. Inset shows synapse indicated by arrow. Scale bar: 5 μM, 2 μM for inset. Plot shows counts for colabeled and partially colabeled elements in the zone of physiological recording (*$p < 0.02$, ANOVA; n = 6/group).

(E and F) YFP-actin-transfected DIV17 neurons were treated for 15 min with 10–70 μM blebbistatin (red, Blebb) or inactive enantiomer (blue) followed by photobleaching (*$p < 0.05$; ANOVA).

(G) Infusions of 0.2 μm jasplakinolide (Jasp; black bar) to slices produced an ~40% reduction in field potential slopes. Stimulus intensity was adjusted (down arrow; break in x axis) to return field response sizes to pre-Jasp baseline.

(H) Local infusions (gray bar) of active (*Blebb;* closed) or inactive (*con*; gray) blebbistatin were applied in the continued presence of Jasp beginning 30 s after TBS (upward arrow). No differences were observed between these groups ($p > 0.05$; RM-ANOVA; n = 6–7/group). Results from experiments performed similarly but in the absence of Jasp (aCSF/Blebb, open; see Figure 4C) are shown for comparison (starting 10 min before TBS; n = 8).

Error bars represent SEM.

while disrupting actin polymerization in this region prevents memory consolidation (Fischer et al., 2004). Because our physiology studies demonstrated the involvement of myosin IIb-mediated dynamic alterations to the actin cytoskeleton during LTP stabilization, we hypothesized that myosin II activity may contribute to the processes that underlie information storage and memory formation in the hippocampus. An ideal method for investigating the molecular mechanisms of memory formation is the use of single-trial contextual fear conditioning in combination with intra-CA1 delivery of in vivo shRNAs. Thus, we performed control studies to ensure that the virus injection procedure and expression of a transgene into the dorsal hippocampus had no effect on contextual memory formation. Thirty days after virus infusion, animals expressing high levels of GFP were trained using our standard contextual fear conditioning paradigm and compared to mock-injected and noninjected control groups. Importantly, we found that the injection procedure and exogenous protein expression have no effect on contextual memory formation in rats (Figure S6). In a separate experiment, animals expressing MyH10 shRNAs demonstrated deficits in freezing behavior during the 24 hr long-term memory (LTM) test when compared to animals expressing control shRNAs (Figures 6A and 6B). In contrast, the behavior of these same animals was no different from controls during the training procedure (Figure 6C). They acquired the context-shock association normally and had comparable levels of exploratory activity. Thus, our data indicate that reduced freezing by animals expressing MyH10-specific shRNAs during the LTM test was not due to state-dependent effects. Together, these data indicate that myosin IIb does not regulate learning but is selectivity involved in stabilizing the acquired contextual association for long-term memory storage.

To further investigate the temporal dynamics of myosin II motor activity in memory formation, we infused Blebb into the hippocampus at various times before and after associative training. Intra-CA1 infusions of Blebb (n = 8 per group) or the control compound (the inactive enantiomer) prior to contextual fear conditioning had no effect on freezing behavior observed during associative training (Figure S7), suggesting that Blebb does not affect an animal's ability to perceive and respond to a footshock. However, Blebb-treated animals displayed dramatically less freezing behavior than their control-treated counterparts during the 24 hr LTM test (Figure 7A), an effect similar to that seen with in vivo shRNAs targeting MyH10 (see Figure 6B). In order to further characterize myosin II's role in memory processes, we next sought to determine if the Blebb-induced memory deficit was due to interference with the acquisition or consolidation of the contextual fear memory. For this

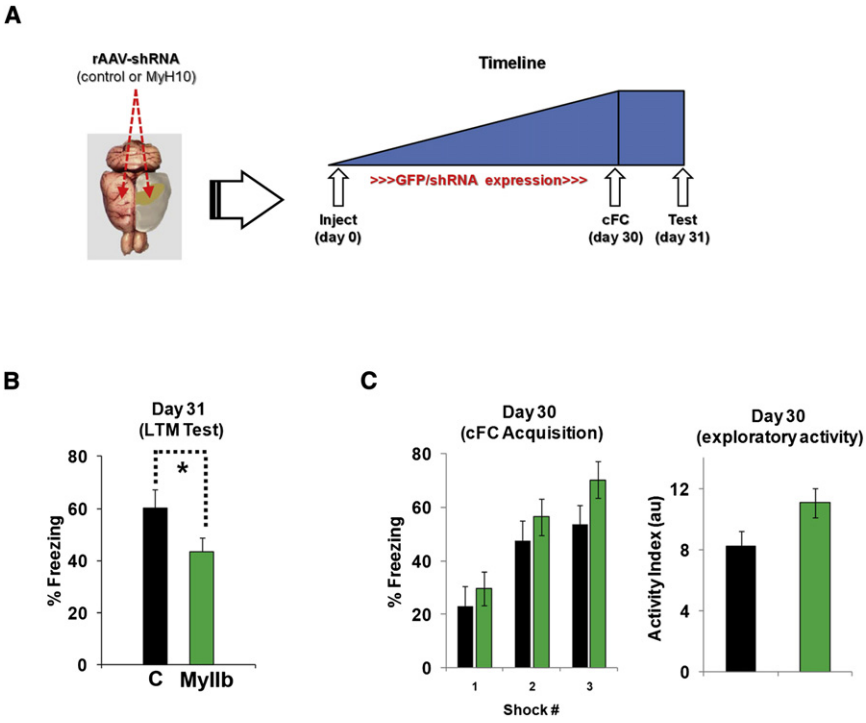

Figure 6. In Vivo Knockdown of the Myosin IIB Motor Impairs Long-Term Memory Formation in the Hippocampus

(A) Experimental design for in vivo knockdown of myosin IIb expression. Animals were injected with rAAV virus particles expressing shRNAs against MyH10 (n = 8) or a control (n = 9), nontargeting shRNA. One month later, all animals were trained for contextual fear conditioning.

(B) In vivo knockdown of MyH10 disrupts normal contextual memory formation as compared to controls ($F_{16} = 4.65$, $^*p < 0.05$).

(C) The left panel shows no difference between groups for post-shock freezing during training, indicating that animals were able to perceive the foot shock, acquire the association and express normal freezing behavior (Post first, second and third shocks, respectively: $F_{16} = 0.440$, $p > 0.05$; $F_{16} = 0.385$, $p > 0.05$; $F_{16} = 2.8$, $p > 0.05$). The right panel shows both groups had comparable exploratory activity during training ($p > 0.05$). Error bars represent SEM.

experiment, animals received the same intra-CA1 infusions 30 min before training but were then tested for short-term memory (STM) 90 min later. Both vehicle and Blebb-treated groups displayed equal expression of the STM (Figure 7B), indicating that acquisition of the novel CS-US association was unaffected by myosin II inhibition. However, the LTM testing of the same animals confirmed our results in Figure 7A, with Blebb-infused animals displaying a LTM deficit (Figure 7B). These results indicate that myosin II activity is important for the consolidation of long-term memories. We next hypothesized that myosin II drives cytoskeletal changes important to LTM formation occurring during, or very shortly after, hippocampus-dependent associative training. Therefore, we sought to determine if myosin II's role in consolidation is restricted to the earliest stages of this process. Remarkably, when delivered just 30 min after training, Blebb had no effect on long-term memory formation when freezing behavior was assessed 24 hr later (Figure 7C). This 30 min posttraining time point is well within the window of protein-synthesis-dependent consolidation mechanisms, indicating that this compound blocks processes during, or immediately after, associative training. Finally, a pretesting infusion of Blebb had no effect on memory expression (Figure S8A). Because CA1 neurons are necessary for the expression of a recent, long-term (24 hr) contextual memory (Anagnostaras et al., 1999; Quinn et al., 2008), these data indicate that Blebb does not block memory consolidation by a nonspecific effect on neuronal firing during associative training.

In our LTP studies, pharmacologically enhancing actin synthesis and filament stability protected synapses from Blebb-induced disruptions. Therefore, we hypothesized that triggering filament polymerization and stabilization prior to conditioning might also prevent Blebb-induced memory disruption. To directly test this idea, we infused JASP, followed by Blebb, into dorsal CA1 and then tested the effects of these agents on LTM. Infusions of JASP into dorsal CA1 prior to contextual fear conditioning did not alter memory formation (Figure 7D). Replicating our earlier finding, treatment with Blebb alone blocked LTM (Figure 7D; see also Figure 7A). When JASP was infused into CA1 45 min before training to drive actin polymerization, myosin II inhibition by Blebb was no longer able to disrupt LTM (Figure 7D). This supports the idea that myosin II motor activity drives actin dynamics that contribute to memory formation. An alternative explanation for this finding is that JASP infusions alter dorsal CA1 in a way that renders it impossible to induce amnesia. To test this possibility, we combined JASP with NMDAR blockade. Contrary to the idea that JASP alters the hippocampus in such a way that memory cannot be disrupted, JASP infusions into dorsal CA1 had no effect on the actions of the amnesia-inducing agent MK-801 (Figure 7E). Because MK-801 blocks memory encoding by inhibiting NMDAR function during memory acquisition, these data indicate that the effects of JASP in dorsal CA1 occur downstream of these receptors. Taken together, our JASP experiments provide excellent evidence that myosin II motor activity drives actin dynamics that subserve contextual memory consolidation.

DISCUSSION

In this study, we demonstrate that myosin II motors mediate a mechanical process that links together LTP induction, F-actin reorganization, and stable synaptic plasticity. We show that LTP induction causes phosphorylation of synaptic MLC. Indeed, this event is the primary means for activating myosin II motor activity and acts as a mechanical force trigger within actin networks (Mogilner and Keren, 2009; Vicente-Manzanares

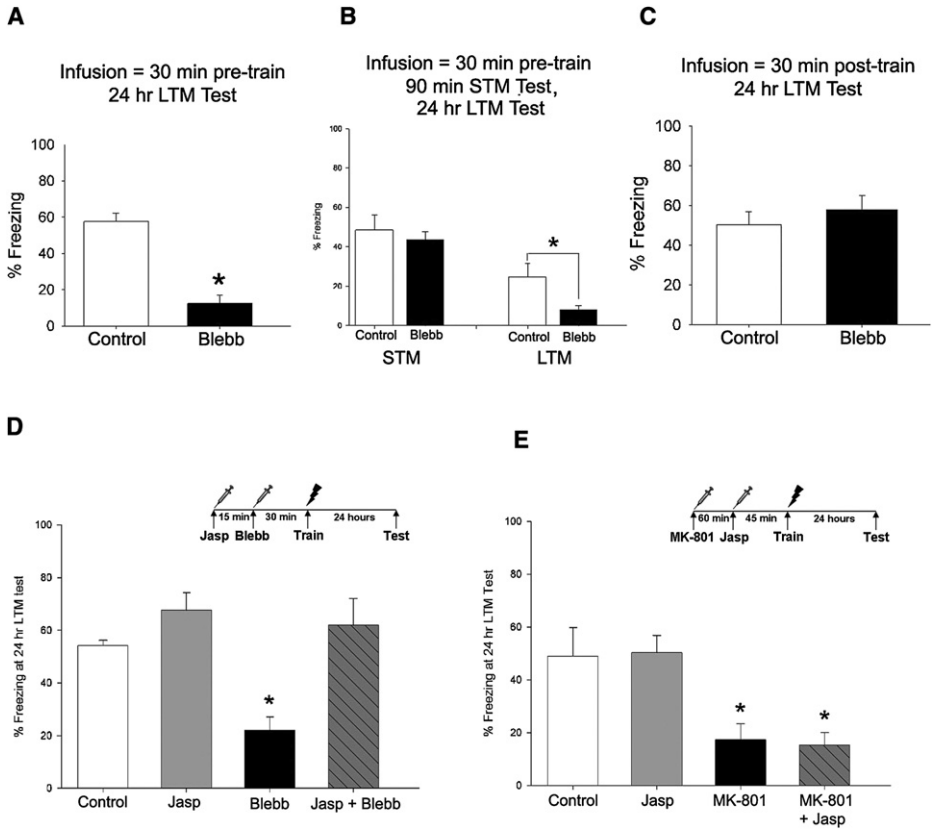

Figure 7. Myosin II Motor Activity Is Required for Memory Consolidation

(A) 30 min pretraining intra-CA1 infusions of Blebb blocked memory formation, as demonstrated by an absence of freezing behavior at the 24 hr test ($F_{15} = 46.91$, $p < 0.001$).

(B) Blebb had no effect on STM assessed 90 min after training, indicating that the Blebb delivered 30 min prior to training does not interfere with memory acquisition ($F_{15} = 0.32$, $p > 0.05$). LTM was assessed in these same animals. Confirming results in (A), Blebb blocked LTM ($F_{15} = 5.02$, $p < 0.05$).

(C) 30 min posttraining intra-CA1 infusions of Blebb had no effect on LTM formation ($F_{14} = 0.71$, $p > 0.05$). Error bars represent SEM.

(D) 45 min pretraining intra-CA1 infusions of Jasp had no effect on LTM ($p > 0.05$), but infusions of Blebb blocked memory formation (*$p < 0.05$), confirming the results depicted in Figure 5. Pretreatment with Jasp occluded the Blebb-induced memory deficit ($p > 0.05$; n = 6/group).

(E) Again, 45 min pretraining intra-CA1 infusions of Jasp alone had no effect on LTM ($p > 0.05$), but injections of MK-801 blocked memory formation ($p < 0.05$). The MK-801-induced memory deficit was maintained when MK-801 treatment was combined with intra-CA1 Jasp infusion ($p < 0.05$; n = 9/group).

Error bars represent SEM.

et al., 2009). Phosphorylation of MLC was dependent upon the activity of NMDARs and the Rho-GTPase-activated kinase, ROCK. We also demonstrate that myosin II activity in the postinduction period was necessary for de novo F-actin structures to appear during LTP induction, indicating that this motor can drive a dynamic process that leads to F-actin synthesis. In support of this idea, the effects of myosin II motor inhibitors were identical to that of the actin polymerization inhibitor, LatA, which also effectively disrupted actin polymerization and LTP stability when applied during the postinduction period. We were able to identify at least one subtype of myosin II involved in this process. In vivo delivery of shRNAs that targeted MyH10, the heavy chain of myosin IIb, prevented F-actin polymerization and stable LTP. Importantly, we also observed a tight correlation between the disruption of filament synthesis and LTP stability in slices expressing MyH10 shRNAs. Finally, preperfusion of the actin polymerizing compound, JASP, blocked the effects of Blebb on LTP stability, confirming that myosin II activity is upstream of F-actin polymerization and LTP stabilization. Our data support a model where myosin II motor activity is enhanced by LTP induction mechanisms in order to forcefully generate de novo actin polymerization. These newly formed filaments appear to stabilize a very early phase of LTP (Figure 8).

How could myosin II, an actin-based motor, contribute to F-actin polymerization in response to LTP induction? In many dynamic cellular structures, such as the leading edge of neuronal growth cones, myosin II is necessary for stimulus-induced F-actin reorganization (Mogilner and Keren, 2009). Importantly, our observations in dendritic spines confirm this may be a ubiquitous role for mammalian myosin II. We do not envision myosin II motor activity as a direct actin synthesis machine. Rather, we see myosin II organizing a complex system of dynamic actin structures through forces applied to F-actin networks, capable of producing de novo filaments upon synaptic stimulation. We

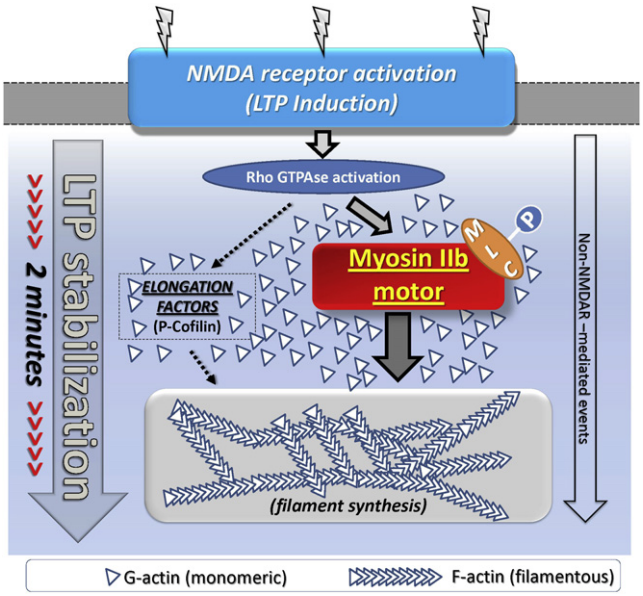

Figure 8. Model of Myosin II-Mediated F-Actin Polymerization in Dendritic Spines

This model outlines a basic mechanism for how LTP induction causes polymerization of the F-actin filaments required to stabilize early LTP at CA1 synapses. Coincident synaptic activity, like that arising from TBS, activates NMDARs leading to the activation of LTP induction mechanisms. LTP induction activates Rho GTPase signaling pathways that target myosin II motors. Activation of myosin II motor activity induces forces within existing actin networks to polymerize F-actin. In addition, we hypothesize that Rho GTPase signaling activates, in parallel, filament elongation mechanisms, such as cofilin phosphorylation. Together, these effectors of the actin cytoskeleton stimulate synthesis of filaments that stabilize a transient increase in synaptic strength to an early form of long-term potentiation.

believe that myosin II-dependent mechanisms work in parallel with the well-described mechanisms that initiate filament elongation. In support of this idea, cofilin, which binds to F-actin to induce depolymerization, is phosphorylated in response to TBS (Chen et al., 2007; Messaoudi et al., 2007) and is required for stable synaptic plasticity (Zhou et al., 2004). This event induces dissociation of cofilin from F-actin and is a candidate mechanism for filament elongation. ROCK inhibition prevents LTP, TBS-induced cofilin phosphorylation and actin filament synthesis (Huang et al., 2007; Rex et al., 2009). Interestingly, ROCK inhibition also prevents myosin phosphorylation, though directly inhibiting myosin II motor activity does not alter cofilin phosphorylation. In addition, we show that NMDAR stimulation leads to the simultaneous phosphorylation of MLC and cofilin. Thus, myosin II and cofilin are both downstream of NMDARs. We speculate that each effector may operate in parallel to produce de novo spine F-actin. While we provide evidence for a direct involvement of myosin II motor activity in the immediate postinduction phase of LTP, future studies will be necessary to determine if cofilin has a similarly direct role in postinduction filament synthesis.

We propose that actin reorganization mechanisms in spines are analogous to those in the tip of growth cones (Lin et al., 1996; Medeiros et al., 2006). In these structures, myosin II motor activity provides the force to break apart large actin bundles that are then depolymerized into free G-actin monomers. This pool of monomers allows elongation of actin bundles at the growing edge of the cone. This cycle of actin depolymerization/polymerization is critically dependent on the "scissor effect" created by myosin II forces imparted onto actin bundles (Medeiros et al., 2006). Importantly, arresting myosin II activity disrupts this "retrograde flow" of actin, actin dynamics are severely altered, and the growth cone subsequently collapses. In spines, we hypothesize that a similar flow of actin exists and that this system is organized by myosin II activity. In support of this idea, we observed a dose-dependent increase in the stable pool of F-actin after acute Blebb treatments, indicating that myosin II imparts forces that constantly destabilize F-actin structures in spines. This function of myosin II could provide a readily accessible pool of G-actin that can be used for rapid filament elongation. Indeed, structural plasticity is dependent on the appearance of distinct F-actin structures in spines (Honkura et al., 2008). Alternatively, it is possible that myosin II-induced severing may provide "seeds" for new filaments to polymerize. In either case, our studies ascribe a mechanical framework to the dynamic nature of actin that is specific to the postinduction phase of LTP and report a mechanism that accounts for F-actin synthesis during LTP.

The early phase of LTP described here is not dependent on new protein synthesis. However, recent studies have indicated that rapid, de novo F-actin polymerization triggered by LTP induction supports stable plasticity many hours later (Kelly et al., 2007; Ramachandran and Frey, 2009). It appears that the consolidation of the early, protein-synthesis-independent phase of LTP to a perpetually stable, protein-synthesis-dependent phase requires de novo actin polymerization at induction. Ramachandran and Frey (2009) report that rapid F-actin polymerization induced by synaptic stimulation serves two distinct roles. One role is to stabilize early LTP, which is consistent with our current results as well as past studies (Krucker et al., 2000). The other role, in contrast, appears to support the eventual capture of plasticity-related proteins that stabilize late-phase LTP. Indeed, blocking actin polymerization during LTP induction prevents proteins from entering spines (Smart et al., 2003). In addition, Kelly et al. (2007) report that PKM ζ, which is required for the maintenance of late-phase LTP, is synthesized more efficiently as a result of actin polymerization induced by high-frequency stimulation. Thus, F-actin formed in response to LTP induction may actually be a collection of distinct functional filament pools, each capable of consolidating unique domains of LTP. Considering that we have discovered a mechanism that triggers F-actin synthesis in response to LTP induction (i.e., myosin II motor activity), it will be of interest to test the impact of altered myosin II motor activity on late-phase LTP. It is possible that myosin II has selective effects on early versus later phases of LTP. It is also possible that the filaments formed by myosin II motor activity eventually capture PRPs, or perhaps control the synthesis of PKM ζ. Thus, myosin II force generation within spines may underlie the transition of LTP from a transient increase in synaptic strength to an enduring form of information storage (Kasai et al., 2010).

Finally, we found that actin/myosin II interactions are necessary during, or shortly after, memory acquisition in the dorsal

hippocampus. Infusing a myosin II inhibitor directly into CA1 before associative training prevents consolidation of contextual fear memory, while application of the inhibitor just 30 min after acquisition has no effect. In addition, shRNAs that target the IIb isoform of myosin also disrupted memory formation, indicating that Blebb is targeting myosin IIb, which in turn disrupts memory. Therefore, myosin II participates in processes that trigger the initial encoding of contextual fear associations. These myosin II-dependent processes appear to involve changes to actin dynamics, as we were able to prevent Blebb-induced memory disruption in vivo by local infusions of the actin-polymerizing agent, JASP. Importantly, JASP treatments by themselves did not alter memory formation, indicating that inducing actin polymerization prior to learning does not strengthen context-shock associations. However, inducing actin polymerization does circumvent the necessity of myosin II function for memory formation. Thus, our data suggest that one function of myosin II in CA1 pyramidal neurons is to facilitate the assembly of actin filaments in response to associative training, which has been shown to be a critical step in the complex processes that support the consolidation of contextual memories (Fischer et al., 2004). Interestingly, shRNAs against myosin IIb and Blebb had similar effects in both LTP and memory assays, and JASP reversed the effects of Blebb on synaptic plasticity and memory consolidation. Thus, it is tempting to speculate that myosin II-driven actin dynamics at CA1 synapses underlies early encoding of memories. Indeed, LTP occurs during hippocampus-dependent associative learning (Fedulov et al., 2007; Whitlock et al., 2006), and reversing LTP in CA1 disrupts expression of hippocampus-specific memories (Pastalkova et al., 2006). Alternatively, it is possible that myosin II has unknown functions at the systems level that account for disruption in hippocampus-dependent memory consolidation. Future investigations will focus on the contribution of myosin II to actin dynamics during the early moments after hippocampus-dependent learning.

In conclusion, our studies provide a mechanism that accounts for the emergence of F-actin structures that stabilize an early stage LTP at CA1 synapses. Myosin II activity during the postinduction phase of LTP is necessary for F-actin synthesis and long-term synaptic plasticity. Myosin II motors are highly regulated by a large number of kinases, many of which are calcium activated (Vicente-Manzanares et al., 2009). Therefore, these complexes may be promising targets for drug discovery efforts aimed at enhancing neural plasticity in patients with memory disorders.

EXPERIMENTAL PROCEDURES

All animal procedures were conducted in accordance with the National Institutes of Health *Guide for the Care and Use of Laboratory Animals* and with protocols approved by the local Institutional Animal Care and Use Committees.

Hippocampal Slices and Electrophysiology

Unless otherwise stated, acute hippocampal slices (350 μm) were cut transverse to the long axis of the hippocampus from adult (4–6 weeks) male Sprague Dawley rats and maintained in an interface chamber as previously described (Rex et al., 2007). For rAAV injection studies, dorsal hippocampal slices were sectioned coronally using a vibratome 30 days after virus injection. The right hemisphere was always injected with virus, while the left hemisphere was always left uninjected (naive). GFP expression in individual slices was rapidly assessed at the time of slice preparation using an Olympus IX-70 inverted epifluroescence microscope. Two or three slices from each hemisphere were distributed across two independent interface chambers so that both injected and naive hemispheres were tested on each chamber. Field synaptic physiology was performed as described (Rex et al., 2009). LTP was induced using theta burst stimulation (ten bursts of four 100 Hz single pulses; 200 ms interburst interval) at Schaffer collateral-CA1 synapses and high-frequency stimulation (100 Hz; 1 s) at mossy fiber-CA3 synapses. Miniature excitatory postsynaptic currents were recorded using standard patch-clamp methods with holding potential at −70 mV. All recordings were performed in the presence of 0.5 μM tetrodotoxin and 50 μM picrotoxin. Analysis of frequency and amplitude was performed automatically using pClamp 10. All data are expressed as means ± SEM in plots, unless stated otherwise.

F-Actin Labeling and Immunofluorescence

In situ labeling of F-actin was performed by applying Alexa Fluor 568-phalloidin (6 μM; Invitrogen) topically to live slices either before or after TBS as shown previously (Rex et al., 2007). This treatment does not disrupt synaptic function or LTP; therefore, this compound is cell permeable but nontoxic at the concentrations used in this study. For virus injection studies, phalloidin was applied (3×, 3 min intervals) at the conclusion of physiological recording (60 min post-TBS). Unless otherwise stated, for combined electrophysiology and microscopy studies, slices were removed from the chamber, fixed, and sectioned as described (Rex et al., 2009). For tissue extraction, slices were submerged in conventional ACSF (Rex et al., 2007) containing 2%–5% Triton X-100, 0.5% paraformaldehyde, and 1 mM phalloidin (Sigma) for 2–10 min at room temperature and then fixed overnight in 4% paraformaldehyde/0.1 M PB containing 1% Triton X-100 and 1 mM phalloidin. Double immunolabeling was performed with anti-p-cofilin (ser3; Abcam) or anti-p-MLC2 (ser19; Cell Signaling) and anti-PSD95 (Thermo Fisher Scientific) as described (Rex et al., 2009).

Z-series photomicrographs (0.2 μm steps) of phalloidin labeling were acquired using a 63× PlanApo objective (NA 1.4) on a Leica DM6000 B microscope (Leica, Bannockburn, IL) equipped with a Hamamatsu ORCA-ER CCD camera. For phalloidin-labeled tissue, Z-stacks were collapsed by extended focal imaging (Microsuite FIVE; Soft Imaging Systems, Lakewood, CO) and intensity levels scaled to values determined for each experiment. For immunolabeled tissue, images were processed by restorative deconvolution (Volocity 5.0, Perkin-Elmer; Rex et al., 2009). Quantification of phalloidin-labeled spines (see Lin et al., 2005a; Rex et al., 2007) or immunolabeled synapses (see Rex et al., 2009) within the zone of stimulated synapses (Rex et al., 2007) was performed by in-house-built software on three serial sections (20 μm) from each slice and averaged to obtain representative values for each slice.

Cannula Implantation, Drug Infusions, and Virus Injections

Animals, cannula implantation, and drug infusions into CA1 were identical to Miller and Sweatt (2007). Rats were housed under 12:12 light/dark cycles, with food and water available ad libidum. To ensure accurate cannula placement, brains were collected after the appropriate memory test. Infusion needle tips were found to be located well within area CA1 in all cannulated animals (Figure S8b).

For intracranial virus injections, 275–300 g male rats (~6 weeks of age) were anesthetized with ketamine (90%) and xylazine (10%) and secured in a Kopf stereotaxic apparatus. A 32 gauge Hamilton syringe was targeted for placement directly into CA1 (AP: −4.56 mm relative to bregma; ML: ±3.0 mm; DV: −3.0, 2.8 mm from skull; Paxinos and Watson, 1998) and lowered to the target coordinate. Animals were injected with 1.0–3.0 μl of recombinant adeno-associated virus (rAAV) expressing either eGFP alone or a short hairpin RNA (shRNA) against MyH10 that also expressed wtGFP. All injections were delivered at a rate of 0.13 μl/min. Following surgery, animals were sutured and returned to their home cage. Animals were allowed 1 month to recover before experimentation.

Design and Packaging of In Vivo shRNAs

See Supplemental Information.

Synaptoneurosomes and Western Blotting

Viable synaptoneurosomes were prepared from forebrain tissue dissected from adult (4–6 weeks old) male Sprague Dawley rats as previously described (Chen et al., 2010). The ROCK inhibitor H1152, or vehicle, was applied to synaptoneurosomes for 10 min immediately followed by NMDA (100 μM) or vehicle for 5 min. Samples were normalized by Bio-Rad protein assay and processed for Western blot analysis (4%–12% gradient SDS-PAGE; Invitrogen) using rabbit antisera to pMLC-s19 (Cell Signaling) or pCofilin-s3 (Abcam) and the ECL Plus detection system (GE Healthcare). Blots were stripped and reprobed for total myosin light chain (Abnova) and bands were measured using ImageJ. Population values represent number of samples tested.

Behavioral Procedures

All animals were handled for 5 days prior to the start of behavioral conditioning. Either 30 min before or 30 min after contextual fear conditioning training, animals received intra-CA1 infusions of the myosin II inhibitor, Blebb, or the appropriate vehicle (inactive Blebb dissolved in 20% DMSO/saline). For experiments that included JASP, animals received infusions of JASP or vehicle (2% DMSO) 45 min prior to training, followed by infusions of Blebb or vehicle (20% DMSO) 15 min later (30 min prior to training). For experiments that included MK-801, injections of MK-801 or saline were delivered 1 hr prior to training, followed by infusions of JASP or vehicle 15 min later. Fear conditioning was performed as described previously (Miller and Sweatt, 2007). Short-term fear memory was assessed 90 min later and long-term fear memory was assessed 24 hr later. For testing, animals were exposed to the context in the absence of footshock for 5 min and freezing was assessed.

Drugs and Stock Solutions

See Supplemental Information.

FRAP Experiments

Medium-density primary hippocampal cultures were prepared from embryonic day 19 (E19) rat embryos as described (Rumbaugh et al., 2006). YFP-β-actin (Clontech) was transfected into cultured neurons and imaged several days later. Two spines were selected on each neuron for photobleaching. Bleaching was performed with the 514 nm line from a 30 mW argon laser coupled to a Zeiss LSM 510 NLO. Confocal imaging of live neurons was done in a plastic culture dish with a 63× plan-Apochromat water-immersion lens (Zeiss; NA 1.0). To determine recovery of fluorescence, we extracted the mean intensity of a region that corresponded to a bleached or unbleached region of interest (to assess bleaching arising from the image series). Images were collected every 10 s. Blebb has been reported to cause toxicity to cells and becomes inactivated when illuminated with <500 nm light (Kolega, 2004; Sakamoto et al., 2005). Thus, all live imaging of neurons in Blebb experiments was performed with either YFP (Ex 514) or mCherry (Ex 543). Second, when Blebb was used in an imaging experiment, we kept the rooms as dark as possible and filtered the bright-field halogen lamp with a long-pass IR filter.

SUPPLEMENTAL INFORMATION

Supplemental Information includes Supplemental Experimental Procedures and eight supplemental figures and can be found with this article online at doi:10.1016/j.neuron.2010.07.016.

ACKNOWLEDGMENTS

We would like to thank Dr. J. David Sweatt for his many helpful discussions and critical evaluation of the manuscript. We would also like to thank Huashi Li, Ryley Parrish, and Anupam Sharma for their support and technical assistance. This work was supported by UAB start-up funds, The McKnight Brain Institute, The Alabama Health Sciences Foundation and National Institute of Neurological Disorders (NINDS) grant NS064079 (G.R), NINDS grants NS05182 (G.L.), and NS45260 (G.L. and C.M.G.). L.Y.C. was supported by National Institute of Mental Health grant MH083396. C.S.R. was supported by National Institute on Aging grant AG00096, NINDS grant 045540, and the Kauffman Foundation. N.M. is an inventor of patents related to rAAV technology and owns equity in a gene therapy company that is commercializing AAV for gene therapy applications.

Accepted: July 13, 2010
Published: August 25, 2010

REFERENCES

Allison, D.W., Gelfand, V.I., Spector, I., and Craig, A.M. (1998). Role of actin in anchoring postsynaptic receptors in cultured hippocampal neurons: differential attachment of NMDA versus AMPA receptors. J. Neurosci. *18*, 2423–2436.

Anagnostaras, S.G., Maren, S., and Fanselow, M.S. (1999). Temporally graded retrograde amnesia of contextual fear after hippocampal damage in rats: within-subjects examination. J. Neurosci. *19*, 1106–1114.

Backouche, F., Haviv, L., Groswasser, D., and Bernheim-Groswasser, A. (2006). Active gels: dynamics of patterning and self-organization. Phys. Biol. *3*, 264–273.

Burger, C., Gorbatyuk, O.S., Velardo, M.J., Peden, C.S., Williams, P., Zolotukhin, S., Reier, P.J., Mandel, R.J., and Muzyczka, N. (2004). Recombinant AAV viral vectors pseudotyped with viral capsids from serotypes 1, 2, and 5 display differential efficiency and cell tropism after delivery to different regions of the central nervous system. Mol. Ther. *10*, 302–317.

Chen, L.Y., Rex, C.S., Casale, M.S., Gall, C.M., and Lynch, G. (2007). Changes in synaptic morphology accompany actin signaling during LTP. J. Neurosci. *27*, 5363–5372.

Chen, L.Y., Rex, C.S., Sanaiha, Y., Lynch, G., and Gall, C.M. (2010). Learning induces neurotrophin signaling at hippocampal synapses. Proc. Natl. Acad. Sci. USA *107*, 7030–7035.

Cheng, X.T., Hayashi, K., and Shirao, T. (2000). Non-muscle myosin IIB-like immunoreactivity is present at the drebrin-binding cytoskeleton in neurons. Neurosci. Res. *36*, 167–173.

Cheng, D., Hoogenraad, C.C., Rush, J., Ramm, E., Schlager, M.A., Duong, D.M., Xu, P., Wijayawardana, S.R., Hanfelt, J., Nakagawa, T., et al. (2006). Relative and absolute quantification of postsynaptic density proteome isolated from rat forebrain and cerebellum. Mol. Cell. Proteomics *5*, 1158–1170.

Correia, S.S., Bassani, S., Brown, T.C., Lisé, M.F., Backos, D.S., El-Husseini, A., Passafaro, M., and Esteban, J.A. (2008). Motor protein-dependent transport of AMPA receptors into spines during long-term potentiation. Nat. Neurosci. *11*, 457–466.

Even-Faitelson, L., Rosenberg, M., and Ravid, S. (2005). PAK1 regulates myosin II-B phosphorylation, filament assembly, localization and cell chemotaxis. Cell. Signal *17*, 1137–1148.

Fedulov, V., Rex, C.S., Simmons, D.A., Palmer, L., Gall, C.M., and Lynch, G. (2007). Evidence that long-term potentiation occurs within individual hippocampal synapses during learning. J. Neurosci. *27*, 8031–8039.

Fischer, A., Sananbenesi, F., Schrick, C., Spiess, J., and Radulovic, J. (2004). Distinct roles of hippocampal de novo protein synthesis and actin rearrangement in extinction of contextual fear. J. Neurosci. *24*, 1962–1966.

Fukazawa, Y., Saitoh, Y., Ozawa, F., Ohta, Y., Mizuno, K., and Inokuchi, K. (2003). Hippocampal LTP is accompanied by enhanced F-actin content within the dendritic spine that is essential for late LTP maintenance in vivo. Neuron *38*, 447–460.

Goeckeler, Z.M., Masaracchia, R.A., Zeng, Q., Chew, T.L., Gallagher, P., and Wysolmerski, R.B. (2000). Phosphorylation of myosin light chain kinase by p21-activated kinase PAK2. J. Biol. Chem. *275*, 18366–18374.

Hirano, K., Hirano, M., and Kanaide, H. (2004). Regulation of myosin phosphorylation and myofilament Ca2+ sensitivity in vascular smooth muscle. J. Smooth Muscle Res. *40*, 219–236.

Holzinger, A. (2009). Jasplakinolide: an actin-specific reagent that promotes actin polymerization. Methods Mol. Biol. *586*, 71–87.

Honkura, N., Matsuzaki, M., Noguchi, J., Ellis-Davies, G.C., and Kasai, H. (2008). The subspine organization of actin fibers regulates the structure and plasticity of dendritic spines. Neuron *57*, 719–729.

Huang, F., Chotiner, J.K., and Steward, O. (2007). Actin polymerization and ERK phosphorylation are required for Arc/Arg3.1 mRNA targeting to activated synaptic sites on dendrites. J. Neurosci. *27*, 9054–9067.

Kasai, H., Fukuda, M., Watanabe, S., Hayashi-Takagi, A., and Noguchi, J. (2010). Structural dynamics of dendritic spines in memory and cognition. Trends Neurosci. *33*, 121–129.

Kelly, M.T., Yao, Y., Sondhi, R., and Sacktor, T.C. (2007). Actin polymerization regulates the synthesis of PKMzeta in LTP. Neuropharmacology *52*, 41–45.

Kolega, J. (2004). Phototoxicity and photoinactivation of blebbistatin in UV and visible light. Biochem. Biophys. Res. Commun. *320*, 1020–1025.

Kramár, E.A., Lin, B., Rex, C.S., Gall, C.M., and Lynch, G. (2006). Integrin-driven actin polymerization consolidates long-term potentiation. Proc. Natl. Acad. Sci. USA *103*, 5579–5584.

Krucker, T., Siggins, G.R., and Halpain, S. (2000). Dynamic actin filaments are required for stable long-term potentiation (LTP) in area CA1 of the hippocampus. Proc. Natl. Acad. Sci. USA *97*, 6856–6861.

Lang, C., Barco, A., Zablow, L., Kandel, E.R., Siegelbaum, S.A., and Zakharenko, S.S. (2004). Transient expansion of synaptically connected dendritic spines upon induction of hippocampal long-term potentiation. Proc. Natl. Acad. Sci. USA *101*, 16665–16670.

Lee, K.S., Schottler, F., Oliver, M., and Lynch, G. (1980). Brief bursts of high-frequency stimulation produce two types of structural change in rat hippocampus. J. Neurophysiol. *44*, 247–258.

Lewis, T.L., Jr., Mao, T., Svoboda, K., and Arnold, D.B. (2009). Myosin-dependent targeting of transmembrane proteins to neuronal dendrites. Nat. Neurosci. *12*, 568–576.

Limouze, J., Straight, A.F., Mitchison, T., and Sellers, J.R. (2004). Specificity of blebbistatin, an inhibitor of myosin II. J. Muscle Res. Cell Motil. *25*, 337–341.

Lin, C.H., Espreafico, E.M., Mooseker, M.S., and Forscher, P. (1996). Myosin drives retrograde F-actin flow in neuronal growth cones. Neuron *16*, 769–782.

Lin, B., Kramár, E.A., Bi, X., Brucher, F.A., Gall, C.M., and Lynch, G. (2005a). Theta stimulation polymerizes actin in dendritic spines of hippocampus. J. Neurosci. *25*, 2062–2069.

Lin, C.Y., Lynch, G., and Gall, C.M. (2005b). AMPA receptor stimulation increases alpha5beta1 integrin surface expression, adhesive function and signaling. J. Neurochem. *94*, 531–546.

Lynch, G., Rex, C.S., and Gall, C.M. (2007). LTP consolidation: substrates, explanatory power, and functional significance. Neuropharmacology *52*, 12–23.

Martin, S.J., Grimwood, P.D., and Morris, R.G. (2000). Synaptic plasticity and memory: an evaluation of the hypothesis. Annu. Rev. Neurosci. *23*, 649–711.

Matsumura, F. (2005). Regulation of myosin II during cytokinesis in higher eukaryotes. Trends Cell Biol. *15*, 371–377.

Matsuzaki, M., Honkura, N., Ellis-Davies, G.C., and Kasai, H. (2004). Structural basis of long-term potentiation in single dendritic spines. Nature *429*, 761–766.

Matus, A. (2000). Actin-based plasticity in dendritic spines. Science *290*, 754–758.

Matus, A., Ackermann, M., Pehling, G., Byers, H.R., and Fujiwara, K. (1982). High actin concentrations in brain dendritic spines and postsynaptic densities. Proc. Natl. Acad. Sci. USA *79*, 7590–7594.

Medeiros, N.A., Burnette, D.T., and Forscher, P. (2006). Myosin II functions in actin-bundle turnover in neuronal growth cones. Nat. Cell Biol. *8*, 215–226.

Messaoudi, E., Kanhema, T., Soulé, J., Tiron, A., Dagyte, G., da Silva, B., and Bramham, C.R. (2007). Sustained Arc/Arg3.1 synthesis controls long-term potentiation consolidation through regulation of local actin polymerization in the dentate gyrus in vivo. J. Neurosci. *27*, 10445–10455.

Miller, C.A., and Sweatt, J.D. (2007). Covalent modification of DNA regulates memory formation. Neuron *53*, 857–869.

Miyazaki, T., Watanabe, M., Yamagishi, A., and Takahashi, M. (2000). B2 exon splicing of nonmuscle myosin heavy chain IIB is differently regulated in developing and adult rat brain. Neurosci. Res. *37*, 299–306.

Mogilner, A., and Keren, K. (2009). The shape of motile cells. Curr. Biol. *19*, R762–R771.

Okamoto, K., Nagai, T., Miyawaki, A., and Hayashi, Y. (2004). Rapid and persistent modulation of actin dynamics regulates postsynaptic reorganization underlying bidirectional plasticity. Nat. Neurosci. *7*, 1104–1112.

Osterweil, E., Wells, D.G., and Mooseker, M.S. (2005). A role for myosin VI in postsynaptic structure and glutamate receptor endocytosis. J. Cell Biol. *168*, 329–338.

Pastalkova, E., Serrano, P., Pinkhasova, D., Wallace, E., Fenton, A.A., and Sacktor, T.C. (2006). Storage of spatial information by the maintenance mechanism of LTP. Science *313*, 1141–1144.

Paxinos, G., and Watson, C. (1998). The Rat Brain in Stereotaxic Coordinates, Fourth Edition (New York: Academic Press).

Quinn, J.J., Ma, Q.D., Tinsley, M.R., Koch, C., and Fanselow, M.S. (2008). Inverse temporal contributions of the dorsal hippocampus and medial prefrontal cortex to the expression of long-term fear memories. Learn. Mem. *15*, 368–372.

Ramachandran, B., and Frey, J.U. (2009). Interfering with the actin network and its effect on long-term potentiation and synaptic tagging in hippocampal CA1 neurons in slices in vitro. J. Neurosci. *29*, 12167–12173.

Rex, C.S., Lin, C.Y., Kramár, E.A., Chen, L.Y., Gall, C.M., and Lynch, G. (2007). Brain-derived neurotrophic factor promotes long-term potentiation-related cytoskeletal changes in adult hippocampus. J. Neurosci. *27*, 3017–3029.

Rex, C.S., Chen, L.Y., Sharma, A., Liu, J., Babayan, A.H., Gall, C.M., and Lynch, G. (2009). Different Rho GTPase-dependent signaling pathways initiate sequential steps in the consolidation of long-term potentiation. J. Cell Biol. *186*, 85–97.

Roman, F., Staubli, U., and Lynch, G. (1987). Evidence for synaptic potentiation in a cortical network during learning. Brain Res. *418*, 221–226.

Rumbaugh, G., Adams, J.P., Kim, J.H., and Huganir, R.L. (2006). SynGAP regulates synaptic strength and mitogen-activated protein kinases in cultured neurons. Proc. Natl. Acad. Sci. USA *103*, 4344–4351.

Ryu, J., Liu, L., Wong, T.P., Wu, D.C., Burette, A., Weinberg, R., Wang, Y.T., and Sheng, M. (2006). A critical role for myosin IIb in dendritic spine morphology and synaptic function. Neuron *49*, 175–182.

Sakamoto, T., Limouze, J., Combs, C.A., Straight, A.F., and Sellers, J.R. (2005). Blebbistatin, a myosin II inhibitor, is photoinactivated by blue light. Biochemistry *44*, 584–588.

Segal, M. (2005). Dendritic spines and long-term plasticity. Nat. Rev. Neurosci. *6*, 277–284.

Sigurdsson, T., Doyère, V., Cain, C.K., and LeDoux, J.E. (2007). Long-term potentiation in the amygdala: a cellular mechanism of fear learning and memory. Neuropharmacology *52*, 215–227.

Smart, F.M., Edelman, G.M., and Vanderklish, P.W. (2003). BDNF induces translocation of initiation factor 4E to mRNA granules: evidence for a role of synaptic microfilaments and integrins. Proc. Natl. Acad. Sci. USA *100*, 14403–14408.

Star, E.N., Kwiatkowski, D.J., and Murthy, V.N. (2002). Rapid turnover of actin in dendritic spines and its regulation by activity. Nat. Neurosci. *5*, 239–246.

Straight, A.F., Cheung, A., Limouze, J., Chen, I., Westwood, N.J., Sellers, J.R., and Mitchison, T.J. (2003). Dissecting temporal and spatial control of cytokinesis with a myosin II Inhibitor. Science *299*, 1743–1747.

Vallee, R.B., Seale, G.E., and Tsai, J.W. (2009). Emerging roles for myosin II and cytoplasmic dynein in migrating neurons and growth cones. Trends Cell Biol. *19*, 347–355.

Vicente-Manzanares, M., Ma, X., Adelstein, R.S., and Horwitz, A.R. (2009). Non-muscle myosin II takes centre stage in cell adhesion and migration. Nat. Rev. Mol. Cell Biol. *10*, 778–790.

Wang, Z., Edwards, J.G., Riley, N., Provance, D.W., Jr., Karcher, R., Li, X.D., Davison, I.G., Ikebe, M., Mercer, J.A., Kauer, J.A., and Ehlers, M.D. (2008). Myosin Vb mobilizes recycling endosomes and AMPA receptors for postsynaptic plasticity. Cell *135*, 535–548.

Whitlock, J.R., Heynen, A.J., Shuler, M.G., and Bear, M.F. (2006). Learning induces long-term potentiation in the hippocampus. Science *313*, 1093–1097.

Zalutsky, R.A., and Nicoll, R.A. (1990). Comparison of two forms of long-term potentiation in single hippocampal neurons. Science *248*, 1619–1624.

Zeng, Q., Lagunoff, D., Masaracchia, R., Goeckeler, Z., Côté, G., and Wysolmerski, R. (2000). Endothelial cell retraction is induced by PAK2 monophosphorylation of myosin II. J. Cell Sci. *113*, 471–482.

Zhang, H., Webb, D.J., Asmussen, H., Niu, S., and Horwitz, A.F. (2005). A GIT1/PIX/Rac/PAK signaling module regulates spine morphogenesis and synapse formation through MLC. J. Neurosci. *25*, 3379–3388.

Zhou, Q., Homma, K.J., and Poo, M.M. (2004). Shrinkage of dendritic spines associated with long-term depression of hippocampal synapses. Neuron *44*, 749–757.